ELSEVIER

Polymer 44 (2003) 1613–1618

polymer

www.elsevier.com/locate/polymer

Effect of the morphology of reactor powders on the structure and mechanical behavior of drawn ultra-high molecular weight polyethylenes

Katherina Tsobkallo[a], Valeria Vasilieva[a], Svetlana Khizhnyak[b], P. Pakhomov[b], V. Galitsyn[c], E. Ruhl[d], V. Egorov[e], A. Tshmel[e,*]

[a]*St. Petersburg State University of Technology and Design, B. Morskaya 18, 191185 St. Petersburg, Russian Federation*
[b]*Department of Physico-Chemistry, Tver' State University, 170002 Tver', Russian Federation*
[c]*Institute of Synthetic Fiber, 170032 Tver', Russian Federation*
[d]*Department of Physics, University Osnabrueck, Barbara str. 7, D-49069 Osnabrueck, Germany*
[e]*Department of Fracture Physics, Loffe Physico-Technical Institute, Russian Academy of Sciences, Polytekhnicheskaya 26, 194021 St. Petersburg, Russian Federation*

Received 15 July 2002; received in revised form 22 November 2002; accepted 7 December 2002

Abstract

Evolution of the straighten-chain-segment length distributions in three polyethylene reactor powders manufactured using different catalysts has been traced through the melting-drawing procedures carried out under the same temperature-deformation conditions. The powders exhibiting the presence of either folded or chain-extended crystalline entities yielded the oriented samples with quantitatively different interfibrillar structure, and, respectively, with different mechanical behavior concluded from their stress–strain curves and variation of the tangential modulus. The correlation between original and final properties of samples derived from reactor powders evidences a persistence of a kind of memory. The longitudinal disorder in nascent chain-extended crystals transforms virtually to the lateral disorder in the axially oriented interfibrillar material.

Keywords: Polyethylene; Reactor powder; Remnant morphology

1. Introduction

An idea to correlate the morphology of the drawn polyethylene to its initial (unoriented) structure, on the one hand, and the mechanical properties to the morphology, on the other hand, is not a novel approach to the problem of manufacturing the high performance polymeric materials, but the search of new potentialities of structural memory mechanisms is an obvious trend in a series of the most recent publications of different research groups working in this area [1–4]. The increasing interest to this problem is caused, to a certain extent, by the emerging of advanced technologies in polyolefine synthesis including the production of high strength and high modulus polyethylene (PE) from reactor powders polymerized under special conditions [5–8].

A primary transformation of the polymer powder to the isotropic material appropriate for applying the drawing procedure, could be performed using various techniques. In earlier work [3] it has been shown that the gel technology deletes almost all the difference in regular structure of nascent powders; in particular, the length distribution of all-*trans* sequences in gel-derived sheets (which is a factor as-affecting the further crystallization process) depends only on the gel preparation prehistory but not on the initial structure of powders. The melt-crystallized (MC) samples prepared from a set of powders exhibited, in contrast, a certain influence of the original structure thus indicating the incomplete structure-memory loss after the applied heat treatment [3]. Therefore one can expect that some powder-related remnant features in the MC preforms would be conserved after the drawing process with the effect on the macroscopic properties of the finished fibers and films.

This work is to find a correspondence between the crystalline structure of the reactor powders and the

* Corresponding author. Tel.: +7-812-3030602; fax: +7-812-2478924.
E-mail address: chmel@mail.ioffe.ru (A. Tshmel).

0032-3861/03/$ - see front matter © 2003 Elsevier Science Ltd. All rights reserved.
PII: S0032-3861(02)00909-6

mechanical behavior of the drawn MC films made of ultra-high molecular weight (UHMW) polyethylenes. In distinction to works where the nascent powders were transformed to highly-oriented specimens with maximum maintenance of their initial morphology (using 'sandwich'-like co-extrusion or similar techniques [9,10]), we applied a routine multi-stage hot drawing. A highly developed partially-ordered interfibrillar phase (called also 'non-crystalline' material [4,11], or 'third component' [12]) is an inevitable attribute of so prepared samples. We offer results that evidence not only the retention of a memory about the virgin powder structure through the entire preparation procedure but demonstrate the effect of its influence on the mechanical properties of the hot-drawn films.

All the powders and oriented samples were characterized by their straight-chain-segment (SCS) length distribution available from the low-frequency Raman spectroscopy, i.e. from the Raman spectra recorded in the range of longitudinal acoustic modes (LAM). This characterization is of particular importance when one aims to reveal any residuals of the primary regularity in the oriented structure [13]. The LAM spectroscopy is sensitive to the regular stems of any kind irrespective of their localization either in the three-dimension crystal, or in the 'bundles' of straighten molecules [14], or in the individual SCS (including the taut-tie molecules (TTM)) situated both in amorphous and crystalline regions.

The mechanical behavior of the samples was learned from the measurements of the strain–stress diagrams (which were then used for receiving the tangential modulus versus strain, E_t versus ε, dependencies).

2. Samples and methods

Three sorts of PE reactor powders were used in the experiments. One of them was prepared using a conventional Ziegler–Natta catalyst whereas two others were synthesized using highly-efficient supported catalysts (Table 1).

The films were obtained by melting the powders at 180 °C for about 10 min with subsequent cooling of the sample in melting ice. The films were drawn up using a multi-stage hot orientation procedure with a repeated stepwise increase of the temperature from 120 to 140 °C. All the samples were of the same draw ratio $\lambda = 6$.

Table 1
Characteristics of samples

Designation	M_W[a]	M_W/M_N	Catalyst	Manufacturer
PE1.7	1.7×10^6	20–22[b]	Conventional	Plastpolymer, Russia
PE3.0	3.0×10^6	~7	Supported	Hoechst, Germany
PE6.2	6.2×10^6	~7	Supported	NKK-Tomsk, Russia

[a] Calculated from the inherent viscosity in decalin at 135 °C.
[b] Material contains about 10% of a $M_w = 10^4$ fraction.

The DCS experiments were performed on a Perkin–Elmer scanning calorimeter Model DSC-2 calibrated with the melting temperatures of indium (429.7 K) and ice (273.1 K) as well as by the heat capacity of sapphire.

The Raman spectra were excited by a 100 mW NdYVO4 laser and recorded with a triple monochromator DILOR XY 800. The spectra of films were excited by the 632.8 nm line of a 50 mW He–Ne laser and detected by a Spex 1401 monochromator, also equipped with a third monochromator. The 90° geometry of the light scattering was used in all experiments; the oriented samples were positioned normally to the inlet slit of the monochromator.

The SCS length distribution was represented by function $F(L)$ giving the average-number fraction of the all-*trans* sequences of length L. As defined in the range of the LAM excitations, the $F(L)$ is corresponded with the Raman intensity, $I(\omega)$, by the relation

$$F(L) \propto I(\omega)[1 - \exp(-hc\omega/kT)]\omega_L^2 \quad (1)$$

where $\omega_L = (2cL)^{-1}(E/\rho)^{1/2}$ is the frequency of acoustic vibrations [15]; c is the speed of light; ρ is the density; E is the Young's modulus in the chain direction.

The mechanical tests were performed with the help of the Instron 1122 machine operating in the tensile mode.

3. Results

3.1. DSC

Fig. 1 presents the DSC thermograms of reactor powders recorded at a heating rate 10 °C/min. The melting peaks are situated at 142.3, 143.3 and 144.5 °C for samples PE3.0, PE1.7 and PE6.2, respectively. The high melting point of the PE6.2 powder evidences indirectly the chain-extended structure of the crystalline phase [16]. The peak position of the PE3.0 powder is more consistent with the lamellar structure. The main peak of the PE1.7 powder occupies an intermediate position; in addition, there is a second peak at 129.5 °C in the PE1.7 powder thermogram. A complicated

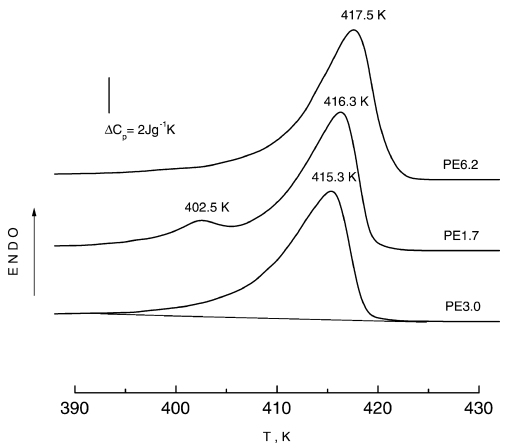

Fig. 1. The DSC thermograms for reactor powders PE3.0, PE1.7 and PE6.2.

character of the DSC thermogram obtained for the PE1.7 can be caused by a wide molecular-weight distribution (MWD) that includes a substantial 'low-molecular' 10^4 fraction.

3.2. SCS

3.2.1. Powders

Fig. 2 shows the original Raman spectra (insets) and calculated SCS length distributions in powders of three sorts. First of all, one should conclude that there is no correlation neither between the M_W and the distribution function $F(L)$, nor between a type of used catalyst and the $F(L)$. Moreover, two one-active-center catalysts (used for manufacturing powders PE3.0 and PE6.2) yield quite different SCS length distributions. Judging from the narrow profile of the $F(L)$, the PE3.0 sample has an ordinary lamellar structure since the thickness of the folded crystals is determined almost completely by the thermodynamical conditions thus being a well-defined parameter. In contrast, the SCS distribution in the PE6.2 powder covers the wide range from ~5 nm to more than 50 nm. It is a distribution of this kind that one could expect in the case of independent chain extending, as this process is strongly influenced by the local synthesis conditions, such as catalyst aging, monomer migration etc. In result, there appears a broad set of variously extended molecules with a length distribution function like seen in Fig. 2(c).

The ordered phase in the PE1.7 powder prepared using a conventional catalyst cannot be unambiguously referred as either lamellar crystals or chain-extended entities. From a comparison of the DSC and Raman data, one can admit that this reactor powder possesses both folded and chain-extended crystalline units. It is worthy to note that two LAM peaks in annealed material prepared from a reactor powder was observed in Ref. [13].

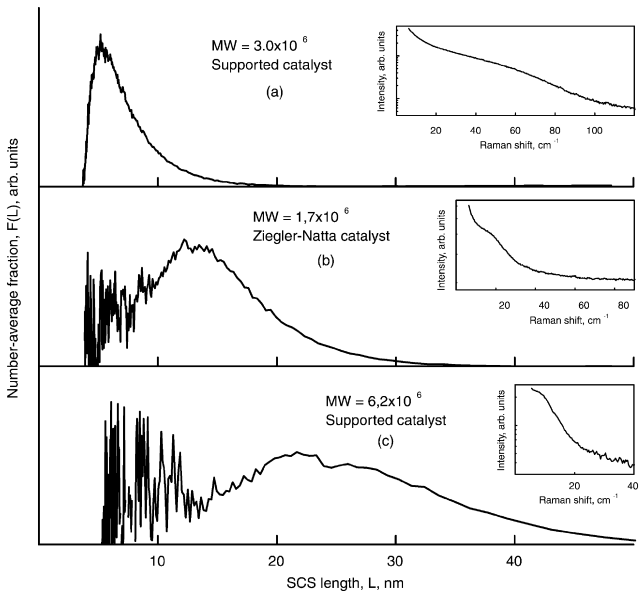

Fig. 2. Low-frequency Raman spectra (insets) and calculated from them SCS length distributions in reactor powders with M_w equal to 3.0×10^6 (a), 1.7×10^6 (b) and 6.2×10^6 (c).

3.2.2. Melt-crystallized

The SCS length distributions in MC samples prepared from the powders are shown in Fig. 3. One can see that the main maxima of the distribution function are situated at ~15 nm in both PE3.0 and PE1.7 samples, with an extra peak appearing at ~10 nm in the latter one. In the PE6.2 sample, the $F(L)$ function peak is situated at ~10 nm, that coincides with the PE1.7 sample extra peak position. Bearing in mind that the crystallite size (L_c) in PE samples prepared from melts under the same conditions is a very stable parameter, and it is independent on the MWD (at least, at $M_W > 10^3$ [17]), we conclude that the main maxima in the SCS length distributions of the PE3.0 and PE1.7 samples belong to the SCS involved in the lamellar crystals of length $L_c = 15$ nm; in the SCS length distribution of the PE6.2 sample, the crystallite maximum is situated at the same position (15 nm) but this is overlapped with the peak at 10 nm which originates from the contribution of regular sequences non-involved in lamellar crystals.

This non-crystalline fraction is not represented at all in the SCS length distribution of a 'fully lamellar' PE3.0 sample; in contrast, the non-crystalline fraction dominates in the SCS length distribution of the PE6.2 sample derived from the powder with the chain-extended morphology; finally, the PE1.7 sample prepared from the powder with, as suggested, both lamellar and chain-extended crystals exhibits a dual morphology.

This interpretation is in accordance with the fact that in the $L > L_c$ region (where the contribution of the non-crystalline SCS diminishes to zero), the $F(L)$ profiles of all three samples are very similar as it one could expect for the SCS length distributions in samples with the same crystallite structure.

3.2.3. Drawn

The $F(L)$ profiles in oriented films are shown in Fig. 4. One can see that the maxima in the samples PE3.0 and PE1.7 are at the same positions and only slightly shifted to the long-lengths side in comparison with their positions in undrawn films (17 nm now against 15 nm prior to drawing).

The PE6.2 sample exhibits a complicated, bimodal $F(L)$ profile. A peak of smaller amplitude is also situated at 17 nm, thus indicating the equality of the dimension of the folded crystals which represent the ordered three-dimensional structure in three drawn films.

In the range $L > L_c$, there are massive shoulders in the SCS length distributions of the PE3.0 and PE1.7 samples, and an intense individual peak in the case of the PE6.2 sample. The lengths of these extra (in relation to 'crystalline' SCS) regular stems fall on the range $L_c < L < 2L_c$. Consequently, the $L > L_c$ SCS cannot be ascribed to the TTM or 'bridging' chains [7], i.e. to all-*trans* sequences

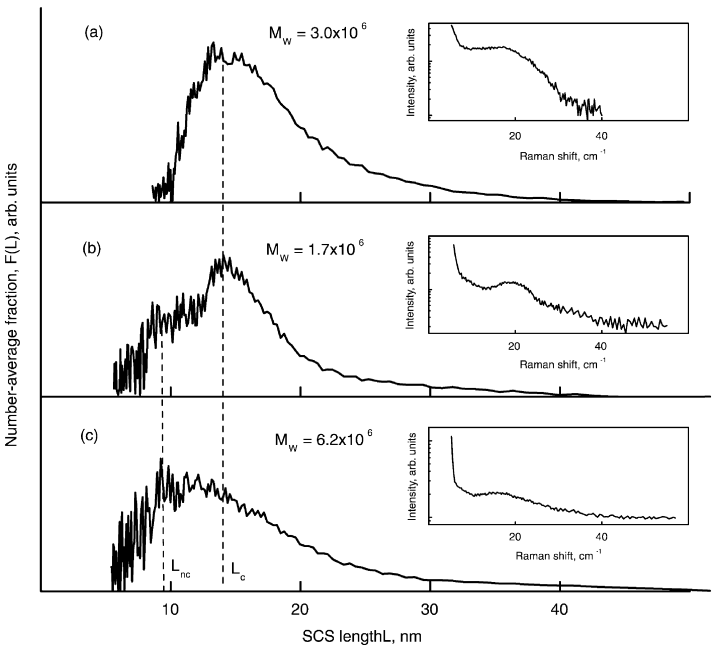

Fig. 3. Low-frequency Raman spectra (insets) and SCS length distributions in MC films PE3.0 (a), PE1.7 (b) and PE6.2 (c); L_{nc} and L_c denote the characteristic lengths of the SCS in non-crystalline phase and in folded crystals, respectively.

passing from one crystallite to another through an intermediate amorphous layer, since the length of the such SCS must exceed $2L_c$. On the other hand, Prevorsek [18] argued for greater length of the interfibrillar regular stems as compared to the intrafibrillar ones. In this light, the observed here $L > L_c$ SCS should be referred to a contribution of the partially ordered interfibrillar phase, more so as the high content of the interfibrillar material aligned with the crystalline component is in agreement with very low values of the ultimate draw ratios of the samples (~ 8).

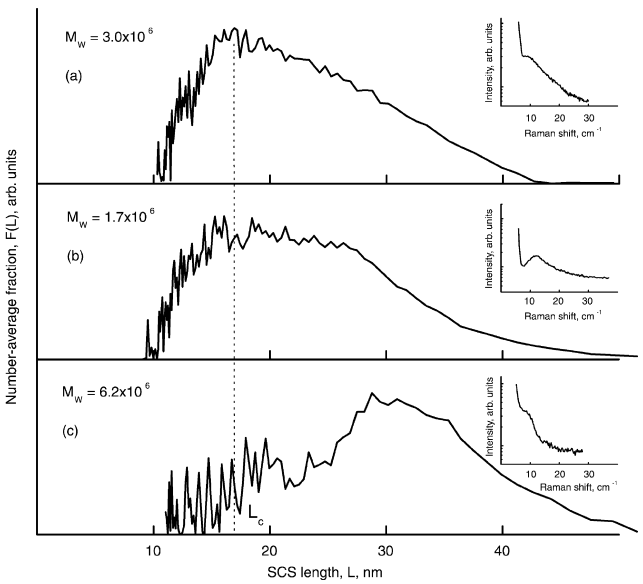

Fig. 4. Low-frequency Raman spectra (insets) and SCS length distributions in $\lambda = 6$ drawn films PE3.0 (a), PE1.7 (b) and PE6.2 (c); L_c denote the characteristic length of the SCS in folded crystals, that is the crystallite size.

3.3. Stress–strain curves

The samples for the mechanical tests were of the same draw ratio and prepared under the identical temperature conditions. In view of the known independence of the mechanical properties on the MWD [7,10], one could expect a similar strain–stress behavior of the samples despite their different origin. At the same time, the draw ratio is not a structural parameter which could be coupled with any particular morphology. Therefore, the limits of Young's modulus versus draw ratio correlation which were established in Refs. [7,10] which are not defined structurally.

Fig. 5 shows the strain–stress curves for oriented films in the full range of deformations. Positive curvature of the initial portions all three plots reflects a trend in the molecular rearrangement to a more uniform stress distribution over chains carrying the load applied. This effect manifests itself more clearly in the E_t versus ε dependences (Fig. 6) calculated from the original σ versus ε curves ($E_t = \partial\sigma(\varepsilon)/\partial\varepsilon$ [19]). The PE6.2 sample demonstrates the lowest values of the tangential modulus on the stage of its

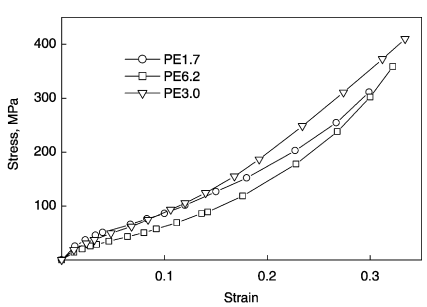

Fig. 5. Stress versus strain curves for $\lambda = 6$ drawn films.

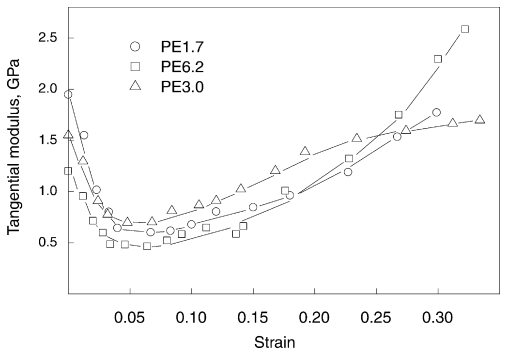

Fig. 6. Tangential modulus versus strain dependencies for $\lambda = 6$ drawn films (calculated from the data shown in Fig. 5).

decrease ($\varepsilon < 5\%$), but the final values obtained for this sample exceed notably those for two other samples.

4. Discussion

A comparison between the SCS length distributions in reactor powders of different morphology and related oriented films allows one to conclude the influence of the nascent chain-extended structure on the morphology of the MC material, and furthermore, on the partially-ordered phase in drawn samples. This kind of the 'memory' about the starting morphology does not imply the conservation of remnant structural units. The correlation between the initial and final morphologies is of virtual character which manifests itself in the mode of the chain-extended crystals decaying when melting. The space between crystalline entities in unoriented material becomes filled with the short regular stems in amount as significant, as these stems yield an individual peak (in addition to the main peak due to the SCS in folded crystals) in the length distribution function (Fig. 3(c)). When drawing, the ensemble of non-crystalline regular stems transforms to the interfibrillar axially ordered SCS which, in turn, exhibit a peak even more intensive than the peak of crystallite-involved all-*trans* sequences (Fig. 4(c)).

In contrast to three-dimensional folded crystals, the chain extended crystals (at least, those that were observed in the PE6.2 powder) possess highly varying stem lengths (Fig. 1(c)), i.e. their lateral order is accompanied with a longitudinal disorder. During the recrystallization in melt, a great part of the chain-extended material transform to the folded structure but debris of the longest extended chains remain uncoiled and fill the interlamellar space after cooling. On the stage of drawing, the spontaneously oriented regular stems, or bundles of stems [14], form the axially extended interfibrillar phase that becomes a prevailing structure in the final product. In other words, the longitudinal disorder in chain extended crystals in powder transforms, finally, to the lateral disorder in the interfibrillar space. At the same time, one should bear in mind that while the chain-extended morphology being true crystalline as formed due to the intermolecular interactions, the preferentially parallel arrangement of the interfibrillar SCS is not supported by bonding of any kind. Therefore, the interfibrillar phase possesses some features inherent in crystals, and other features typical for amorphous regions. Issuing from the geometrical representation of the interfibrillar phase, one should expect that, first, its all-*trans* sequences have a length variation much more significant than those involved in folded crystals and, second, their averaged length exceeds the crystallite size [18]. These two properties of the interfibrillar phase are clearly seen in the SCS length distributions of all our drawn samples being the most pronounced in the film that possessed the chain-extended structure in its prehistory (PE6.2), where the number of the SCS situated in the interfibrillar space exceeds the number of the SCS involved in folded crystallites.

The mechanical behavior of these samples is determined by not the stress-over-TTM distribution in the intercrystalline regions as it takes place in samples with high draw ratio [19,20], but by the lateral disorder in the interfibrillar space. At the first stage of the deformation process, the mobility of non-linked SCS of quite diverse lengths permits their easy longitudinal movement with additional chain-straightening up to the appearance of the tension which at subsequent stage of the deformation would lay obstacle for the slippage of fibrillae. At the same time, the partially ordered material in the interfibrillar space incapable to provide the stress-over-chain distribution as uniform as the intrafibrillar TTM do. Correspondingly, the PE6.2 sample which has the most developed third component exhibits lower values of the tangential modulus on the first stage of the deformation as compared to two other samples.

The second portion of the σ versus ε curves (and related E versus ε dependences) is characterized by the gradual increase of the Young's modulus due to more uniform stress distribution resulted from the straightening of both the TTM and fixed-ends interfibrillar SCS. Under conditions of restricted axial mobility of fibrilla, what is specific for UHMW PE, the presence of an excess of straightened chains in the interfibrillar space becomes an advantage (in the sense of achieving higher values of E). The final (ultimate) value of the Young's modulus of the PE6.2 sample is half as much again as that of two other samples.

The independence of the Young's modulus on the MWD was declared as early as in seventies [10] and confirmed nowadays in the experiments with advanced materials prepared from different reactor powders with both ordinary and particular morphologies [7]. Ward and co-workers [21] argued against the correlation between the Young's modulus and the initial morphology of polymers. They stressed a one-dimensional character of the memory mechanism, thus rejecting an idea about the influence of the internal morphology of reactor powder on the final properties of oriented product, including its mechanical behavior [7].

However, the cited experiments [7,10,21] were carried

out using the highly drawn fibers whose excellent drawability was conditioned by a reduced entanglement density specific for UHMW PE prepared from dilute solutions, gels, or reactor powders compacted and drawn applying a special two-stage orientation procedure [9]. Under these conditions, the tensile modulus is determined by, first of all, the structure of intercrystallite amorphous layers which is highly sensitive to the orientation process [19,20]. An ordered part of the simplest two-component structure, i.e. a crystalline component, is a product of the thermodynamical conditions, and not of the M_W – or even MWD-related properties.

In the presence of the axially ordered interfibrillar phase, the mechanical response of the material to the mechanical loading is not determined by the structure of the true amorphous (intercrystallite) layers only. The SCS that link the fibrillae, participate substantially in the external-stress distribution over individual chains thus affecting the sample behavior during the strain–stress tests. In result, the samples with the same draw ratio but different SCS length distribution in the interfibrillar space exhibit the dependence of the σ versus ε curve (and, to some extent, of the Young's modulus) on some quantitative characteristics of the third component, such as the total number of the SCS and their length distributions.

To conclude, the mechanical properties of the drawn semi-crystalline polymers are dependent on the stress-over-individual SCS distribution irrespective of their localization inside or outside the fibrillae.

5. Summary

The highly developed interfibrillar phase in the UHMW PE films reminiscent of chain-extended morphology of reactor powder affects the mechanical behavior of the samples. The mechanism of the memory is corresponded with the longitudinal disorder in nascent chain-extended crystals which transforms, finally, to the lateral disorder in the axially oriented interfibrillar material.

References

[1] Amornsakchai T, Bassett DC, Olley RH, Unwin AP, Ward IM. Polymer 2001;42:4117–26.
[2] Simon LC, de Souza RF, Soares JBP, Mauler RS. Polymer 2001;42:4885–92.
[3] Pakhomov PM, Khizhnyak S, Galytsyn V, Ruhl E, Vasil'eva V, Tshmel A. J Macromol Sci, Phys 2002;B41:229–40.
[4] Fu Y, Chen W, Pyda M, Londono D, Annis B, Boller A, Habenschuss A, Cheng J, Wunderlich BJ. J Macromol Sci, Phys 1996;B35:37–87.
[5] Pawlikowiski GT, Mitchell DJ, Porter RS. J Polym Sci, Polym Lett Ed 1988;26:1865–72.
[6] Smith P, Chanzy HD, Rotzinger B. Polymer 1989;60:1814–9.
[7] Al-Hussein M, Davies GR, Ward IM. Polymer 2001;42:3679–86.
[8] Sano A, Iwanami Y, Matssura K, Yokoyama S, Kanamoto T. Polymer 2001;42:5859–66.
[9] Kanamoto T, Ohama T, Tanaka K, Takeda M, Porter RS. Polymer 1987;28:1617–23.
[10] Zachariades AE, Kanamoto T. In: Zachariades AE, Porter RS, editors. High modulus polymers: approaches to design and development. New York: Marcel Dekker; 1988.
[11] Prasad K, Grubb D. J Polym Sci 1989;B27:381–92.
[12] Baker AME, Windle AH. Polymer 2001;42:667–80.
[13] Wang LH, Porter RS, Stidham HD, Hsu SL. Macromolecules 1991;24:5535–8.
[14] Ginzburg BM, Shepelevskii AA, Sultanov N, Tuichiev S. J Macromol Sci, Phys 2002;B41:357–87.
[15] Schaufele RF, Schimanouchi T. J Chem Phys 1967;47:3605–12.
[16] Han KS, Wallage JF, Truss RW, Geil PH. J Macromol Sci, Phys 1981;B19:313–49.
[17] Barham A, Keller A. J Mater Sci 1976;11:27–36.
[18] Prevorsek DC. J Macromol Sci 2002;9:733–42.
[19] Schultze-Gebhardt F. Faserforsch Textiltechn 1977;28:467–75.
[20] Pakhomov PM, Shablygin MV, Tsobkallo KS, Chegolya AS. Vysokomol. Soed 1986; 28A, 558–563, In Russian.
[21] Amornsakchai T, Olley RH, Bassett DC, Al-Hussein MOM, Unwin AP, Ward IM. Polymer 2000;41:8291–8.